AIP Journal of Applied Physics

Anharmonicity and necessity of phonon eigenvectors in the phonon normal mode analysis

Tianli Feng, Bo Qiu, and Xiulin Ruan

Citation: Journal of Applied Physics **117**, 195102 (2015); doi: 10.1063/1.4921108
View online: http://dx.doi.org/10.1063/1.4921108
View Table of Contents: http://scitation.aip.org/content/aip/journal/jap/117/19?ver=pdfcov
Published by the AIP Publishing

JOURNAL OF APPLIED PHYSICS **117**, 195102 (2015)

Anharmonicity and necessity of phonon eigenvectors in the phonon normal mode analysis

Tianli Feng, Bo Qiu, and Xiulin Ruan[a)]
School of Mechanical Engineering and the Birck Nanotechnology Center, Purdue University, West Lafayette, Indiana 47907-2088, USA

(Received 26 March 2015; accepted 2 May 2015; published online 18 May 2015; corrected 21 May 2015)

It is well known that phonon frequencies can shift from their harmonic values when elevated to a finite temperature due to the anharmonicity of interatomic potential. Here, we show that phonon eigenvectors also have shifts, but only for compound materials in which each atom has at least two types of anharmonic interactions with other atoms. Using PbTe as the model material, we show that the shifts in some phonon modes may reach as much as 50% at 800 K. Phonon eigenvectors are used in normal mode analysis (NMA) to predict phonon relaxation times and thermal conductivity. We show, from both analytical derivations and numerical simulations, that the eigenvectors are unnecessary in frequency-domain NMA, which gives a critical revision of previous knowledge. This simplification makes the calculation in frequency-domain NMA more convenient since no separate lattice dynamics calculations are needed. On the other hand, we expect our finding of anharmonic eigenvectors may make difference in time-domain NMA and other areas, like wave-packet analysis.
 [http://dx.doi.org/10.1063/1.4921108]

I. INTRODUCTION

Recently, great effort has been made on the prediction of the thermal conductivity κ in general materials as the study of thermal transport has extensive applications in the areas of thermal management and thermoelectrics.[1,2] High-κ materials can help dissipate heat rapidly in packed electronic devices, while low κ is desired for high figure of merit ZT in thermoelectrics. To successfully manage thermal transport in thermal and thermoelectric materials, a deep understanding of the spectral phonon properties is critically important.

Many numerical methods have been developed to predict thermal conductivity.[2] The Green-Kubo (GK) method[3] based on molecular dynamics (MD) simulations has been widely applied to estimate thermal conductivity, but it gives limited insight of phonon properties. The anharmonic lattice dynamics (ALD), presented by Maradudin and the co-workers,[4,5] and its iterative scheme, first proposed by Omini and Sparavigna,[6,7] give the spectral phonon relaxation time, mean free path, and κ. However, they ignore higher order phonon scattering and thus only works well for low temperature. Phonon normal mode analysis (NMA) can include the full anharmonicity of interatomic potential in MD simulations, while it is based on classical thermodynamics so only appropriate for high temperature. The time-domain NMA was proposed by Ladd *et al.*[8] and extended by McGaughey and Kaviany.[9] The frequency-domain NMA, so called spectral energy density (SED) analysis, was early implemented by Wang *et al.*,[10] and then extended by Shiomi and Maruyama,[11] De Koker,[12] and Thomas *et al.*[13,14]

Although NMA has been widely used for predicting phonon relaxation time and thermal conductivity,[8,9,11–21] there are still opening issues to be resolved, and here, we target two of them. First, although it is well known that at finite temperature, the anharmonicity of interatomic potential can lead to phonon frequencies shift from the harmonic values at 0 K, its impact on the phonon eigenvectors has not been examined yet. Second, two versions of frequency-domain NMA, with and without eigenvectors, have been widely used, but there is still a debate whether they are equivalent.[21] In this letter, we first illustrate the harmonic eigenvector (HEVs) and anharmonic eigenvector (AEVs) for one-dimensional (1D) atomic chain and then extended to three-dimensional (3D) bulk materials. After that, we compare the two versions of frequency-domain NMA analytically and numerically.

II. EXISTENCE OF ANHARMONIC EIGENVECTORS

In Fig. 1, we show a diatomic chain with the two atomic masses m_1 and m_2 and two force constants Γ_1 and Γ_2. The lattice constant is a. From lattice dynamics, the diatomic chain has two phonon branches, acoustic and optical, with the eigen-frequencies $\omega_\pm$

$$\omega_\pm^2 = (2m_1m_2)^{-1}[(m_1+m_2)(\Gamma_1+\Gamma_2) \pm \sqrt{(m_1+m_2)^2(\Gamma_1+\Gamma_2)^2 - 8\Gamma_1\Gamma_2(1-\cos ka)m_1m_2}] \quad (1)$$

and the two orthonormal eigenvectors $\mathbf{e}_+ = (e_1,\ e_2)$ and $\mathbf{e}_- = (-e_2^*, e_1^*)$, where k indicates the amplitude of the wave vector $\mathbf{k}$, the subscript "−" denotes the acoustic branch and "+" denotes the optical branch. Considering that the eigenvectors can be multiplied by any arbitrary phase $\exp(i\phi)$, which does not matter the physical meaning of the eigenvectors, thus we only care about the amplitude of the two components, $|e_1|$ and $|e_2|$, which can be viewed as the weights of the phonon normal mode projections on the two basis atoms

[a)]Electronic mail: ruan@purdue.edu

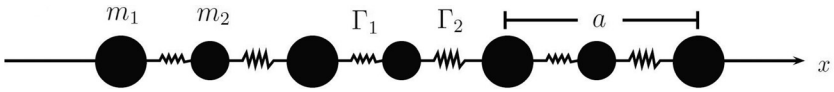

FIG. 1. The sketch of a diatomic chain.

m_1 and m_2, respectively. Since $|e_1|^2 + |e_2|^2$ is normalized as unit, the only quantity that matters is the ratio between them

$$\frac{|e_2|}{|e_1|} = \frac{\sqrt{(1+\eta)^2(1+\xi)^2 - 8\eta\xi(1-\cos ka)} + (1-\eta)(1+\xi)}{2\sqrt{(1+\xi)^2 - 2\xi(1-\cos ka)}}, \tag{2}$$

which is a function that depends on the mass ratio $\eta = m_1/m_2$ and the spring constant ratio $\xi = \Gamma_1/\Gamma_2$.

A. Anharmonic frequencies

In anharmonic systems at finite temperatures, instead of staying at their equilibrium positions, the atoms vibrate around them, and thus, the force constants do not remain at their harmonic values and typically shift down. As a result, the phonon frequencies suffer an anharmonic effect and become lower than their harmonic values at 0 K as the temperature rises. Mathematically, it is seen that the frequencies $\omega_\pm$ decrease with decreasing force constants Γ_1 and Γ_2 in Eq. (1).

B. Anharmonic eigenvectors

In contrast with frequencies, eigenvectors typically have no anharmonic effect since commonly in a diatomic chain the two force constants are equal to each other, $\Gamma_1 = \Gamma_2 = \Gamma$, and thus, $|e_1|/|e_2|$ has no dependence on Γ based on Eq. (2). More generally, $|e_1|/|e_2|$ does not depend on the force constants if $\Gamma_1/\Gamma_2 = Const.$ or $m_1/m_2 = 1$. In other words, for 1D diatomic chain, the eigenvectors will show anharmonic effect at finite temperature only in the conditions that (I) the system contains at least two types of atoms and that (II) each atom has different anharmonic interactions with other atoms.

To investigate if the conclusion is applicable for 3D systems, we conduct lattice dynamics (LD) calculations and MD simulations for several bulk materials, which are divided into three categories. For simplicity, we discuss the eigenvectors of the longitudinal modes first. The first category is the elementary substance (e.g., argon, diamond, silicon, and germanium), which does not satisfy condition I. The second category is the compound material with each atom affected by only one type of interatomic force (e.g., β—SiC), as shown in Fig. 2(a), which does not satisfy condition II. And the last category satisfies both, like PbTe in Fig. 2(b). We first calculate the phonon eigenvectors from harmonic lattice dynamics at 0 K using GULP.[22] Then, we implement MD simulation (by LAMMPS[23]) at finite temperature and calculate eigenvectors using the Green's function method proposed by Kong.[24] The domain sizes for all the bulk systems are $8 \times 8 \times 8$ unit cells (typically 2048 atoms for Ar and 4096 atoms for C, Si, Ge, SiC, and PbTe). Since periodic boundary conditions are applied to the simulation domain, we can resolve 9 **k** points in the [1, 0, 0] direction with reduced wave vector of $k^* = (j/8, 0, 0)$, where j is an integer from 0 to 8. In the Green's Function calculation at Gamma point, we have used 20 iteration steps to enforce the acoustic sum rule and have obtained the phonon frequencies and eigenvectors that match well with LD calculations.

For the first category, the LD calculation and MD simulations show that the eigenvectors of these materials are constants, e.g., the eigenvector of argon bulk (systems with one basis atom in a primitive cell) is $\mathbf{e} = (e, 0, 0)$ with $|e| = 1$; the eigenvector of diamond, silicon, and germanium bulks (systems with two basis atoms in a primitive cell) is $\mathbf{e} = (e_1, 0, 0; e_2, 0, 0)$ with $|e_1| = |e_2| = 1/\sqrt{2}$. As for β—SiC in the second category, as suggested by Porter *et al.*,[25,26] each Si/C atom only has interaction with the four nearest C/Si neighbors by setting cutoff distance for both Si-Si and C-C interactions as 2.56 Å in the Tersoff potential.[27,28] Thus, each atom is affected by only one type of anharmonic force. The results show that HEVs and AEVs are exactly the same, no matter how high temperature is used in MD simulations.

As for bulk PbTe in category 3, each Pb/Te atom has interactions with Pb/Te and Te/Pb atoms that are farther than the nearest neighbors as shown in Fig. 2(b), and these interactions have different anharmonicities.[15] Each basis atom experiences two or multiple types of interactions just like Γ_1 and Γ_2 in the 1D chain case. Expressing the eigenvectors of LA mode as $(e_{Pb}, 0, 0; e_{Te}, 0, 0)$, the ratio between $|e_{Te}|$ and $|e_{Pb}|$ is plotted in Fig. 3 at different temperatures. It is seen that the eigenvectors at 20 K are very close to the harmonic values at 0 K. As the temperature increases, the eigenvectors shift away from HEVs with a considerable difference that is as much as 50% at medium-frequency range. At high temperatures, the equilibrium distances between atoms deviate from their low temperature values due to thermal expansion. As a result, the second order derivatives of the interatomic potential, i.e., force constants at those changed distances are different from their original values. These in turn lead to the change in phonon eigenvectors for materials of category 3 in this paper. We note that the mid-to-high frequencies have more deviations than low frequencies in Fig. 3. A rough

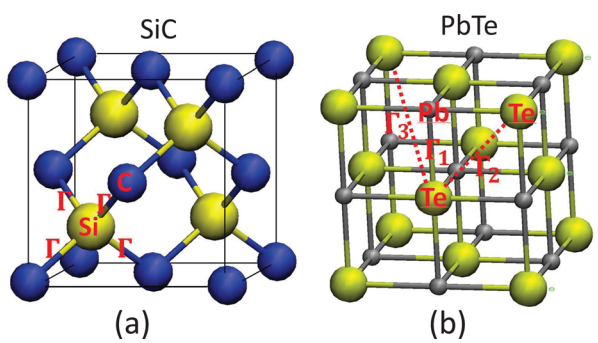

FIG. 2. The sketches to illustrate the interatomic interactions in (a) SiC and (b) PbTe. In SiC, each Si(C) atom has only one type of interaction with the surrounding atoms. In PbTe, each Pb(Te) atom has more than one interactions with the surrounding atoms due to the long range potential.

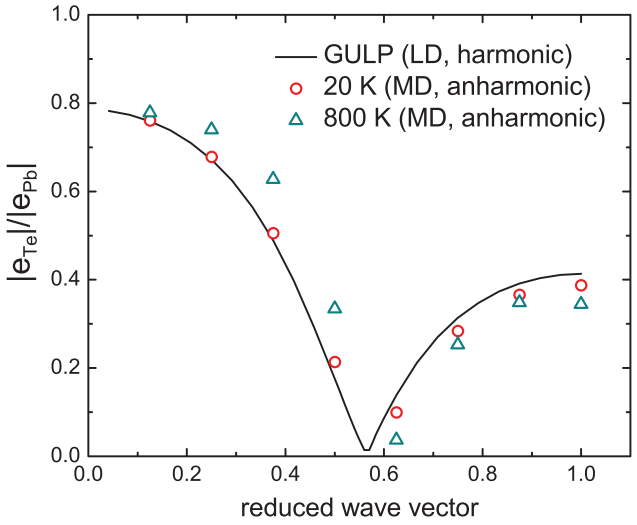

FIG. 3. The ratio $|e_{Te}|/|e_{Pb}|$ as a function of reduced wave vector in the [1, 0, 0] direction for the LA mode of bulk PbTe at different temperatures, where $|e_{Te}|$ and $|e_{Pb}|$ are the moduli of the components of the eigenvector $(e_{Pb}, 0, 0; e_{Te}, 0, 0)$.

explanation is given in Eq. (2) that the value of $|e_1|/|e_2|$ for high k is more sensitive than for small k to the change of ξ, since it seen that $|e_1|/|e_2|$ is even independent on ξ when k approaches zero. Physically, low-frequency phonons with wavelength much longer than the bond length will "view" the material as a continuum and will not sense the difference between Γ_1 and Γ_2 on an atom from its neighbors. For better accuracy, the simulations have been conducted three times for each temperature, and only less than 1% difference between each time is found, which indicates that the differences between HEVs and AEVs are stable and not caused by noises. We note that not only PbTe but also other thermoelectric materials such as PbSe and Bi_2Te_3 have AEVs at finite temperature since they all satisfy the two conditions listed above. Although all the analysis above is done for longitudinal mode, the conclusion also works for transverse modes by similar analysis. By directly calculating and comparing the HEVs and AEVs for transverse modes in the materials, we confirmed this point.

III. NECESSITY OF EIGENVECTORS IN NORMAL MODE ANALYSIS

Eigenvectors are required in normal mode analysis for predicting spectral phonon relaxation time and mean free path.[2] In solids, the vibrations of atoms in real space are represented by the time dependent normal mode coordinates[29]

$$\begin{aligned} q_{\mathbf{k},\nu}(t) &= \sum_{\alpha}^{3}\sum_{b}^{n}\sum_{l}^{N_c}\sqrt{\frac{m_b}{N_c}}u_{\alpha}^{l,b}(t)e_{\alpha}^{b*}(\mathbf{k},\nu)\exp\left(i\mathbf{k}\cdot\mathbf{r}_0^l\right) \\ &= \sum_{\alpha}^{3}\sum_{b}^{n}e_{\alpha}^{*b}(\mathbf{k},\nu)\sum_{l}^{N_c}\sqrt{\frac{m_b}{N_c}}u_{\alpha}^{l,b}(t)\exp\left(i\mathbf{k}\cdot\mathbf{r}_0^l\right) \\ &= \sum_{\alpha}^{3}\sum_{b}^{n}e_{\alpha}^{*b}(\mathbf{k},\nu)q_{\alpha}^{b}(\mathbf{k},t), \end{aligned} \tag{3}$$

where

$$q_{\alpha}^{b}(\mathbf{k},t) = \sum_{l}^{N_c}\sqrt{\frac{m_b}{N_c}}u_{\alpha}^{l,b}(t)\exp\left(i\mathbf{k}\cdot\mathbf{r}_0^l\right). \tag{4}$$

Here, $u_{\alpha}^{l,b}$ is the αth component of the displacement of the bth basis atom in the lth unit cell, e^* is the complex conjugate of eigenvector component, $\mathbf{r}_0^l$ is the equilibrium position of the lth unit cell, ν denotes phonon branch, and n and N_c are the numbers of total basis atoms and total unit cells, respectively. At small perturbation, the normal mode has a frequency shift $\Delta_{\mathbf{k},\nu}$ and linewidth $\Gamma_{\mathbf{k},\nu}$ with the perturbed form[8]

$$q_{\mathbf{k},\nu}(t) = q_{\mathbf{k},\nu,0}\exp\left[i(\omega_{\mathbf{k},\nu}^{A} + i\Gamma_{\mathbf{k},\nu})t\right], \tag{5}$$

where $q_{\mathbf{k},\nu,0}$ is the vibration amplitude, a constant for a given mode $(\mathbf{k}, \nu)$; $\omega_{\mathbf{k},\nu}^{A}$ is the anharmonic frequency with $\omega_{\mathbf{k},\nu}^{A} = \omega_{\mathbf{k},\nu} + \Delta_{\mathbf{k},\nu}$.

In the time-domain NMA method,[8,9] the spectral phonon relaxation time $\tau_{\mathbf{k},\nu}$ is obtained by fitting the autocorrelation function

$$\frac{\langle E_{\mathbf{k},\nu}(t)E_{\mathbf{k},\nu}(0)\rangle}{\langle E_{\mathbf{k},\nu}(0)E_{\mathbf{k},\nu}(0)\rangle} = \frac{\int_0^{\infty}E_{\mathbf{k},\nu}(t'+t)E_{\mathbf{k},\nu}(t')d\xi}{\int_0^{\infty}E_{\mathbf{k},\nu}(t')E_{\mathbf{k},\nu}(t')dt'} = e^{-t/\tau_{\mathbf{k},\nu}} \tag{6}$$

as an exponential decay form. Here,

$$E_{\mathbf{k},\nu}(t) = \frac{\omega_{\mathbf{k},\nu}^2|q_{\mathbf{k},\nu}(t)|^2}{2} + \frac{|\dot{q}_{\mathbf{k},\nu}(t)|^2}{2} \tag{7}$$

is the total energy of the mode $(\mathbf{k}, \nu)$. Besides the trajectory of each atom, the method requires the eigenvectors to evaluate normal mode amplitude in Eq. (3).

The frequency-domain NMA methods have two different formalisms. The first one is to calculate the total spectral energy density (SED) $(\Phi(\mathbf{k}, \omega))$ for a given $\mathbf{k}$ by summing up the SED's of all the phonon branches $(\Phi_\nu(\mathbf{k}, \omega))$

$$\begin{aligned} \Phi(\mathbf{k},\omega) &= \sum_{\nu}^{3n}\Phi_{\nu}(\mathbf{k},\omega) = \sum_{\nu}^{3n}|\dot{q}_{\mathbf{k},\nu}(\omega)|^2 \\ &= \sum_{\nu}^{3n}\left|\sum_{\alpha}^{3}\sum_{b}^{n}e_{\alpha}^{*b}(\mathbf{k},\nu)\,\dot{q}_{\alpha}^{b}(\mathbf{k},\omega)\right|^2, \end{aligned} \tag{8}$$

where

$$\begin{aligned} \Phi_{\nu}(\mathbf{k},\omega) &= |\dot{q}_{\mathbf{k},\nu}(\omega)|^2 = \left|\int_0^{+\infty}\dot{q}_{\mathbf{k},\nu}(t)e^{-i\omega t}\mathrm{d}t\right|^2 \\ &= \frac{C_{\mathbf{k},\nu}}{\left(\omega-\omega_{\mathbf{k},\nu}^{A}\right)^2+\Gamma_{\mathbf{k},\nu}^2}. \end{aligned} \tag{9}$$

$\Phi_\nu(\mathbf{k}, \omega)$ is the Fourier transform of the time derivative of $q_{\mathbf{k},\nu}(t)$, $C_{\mathbf{k},\nu} = (\omega_{\mathbf{k},\nu}^{A2} + \Gamma_{\mathbf{k},\nu}^2)q_{\mathbf{k},\nu,0}^2$ is a constant related to $(\mathbf{k}, \nu)$. By fitting Eq. (8) as $3n$ Lorentzian functions, the peak positions $\omega_{\mathbf{k},\nu}^{A}$ and full widths at half maximum $2\Gamma_{\mathbf{k},\nu}$ as well as phonon relaxation time $\tau_{\mathbf{k},\nu} = 1/2\Gamma_{\mathbf{k},\nu}$ are obtained. Contrast to the first version, the second one is to calculate the total SED without evaluating the SED of each branch[11–13]

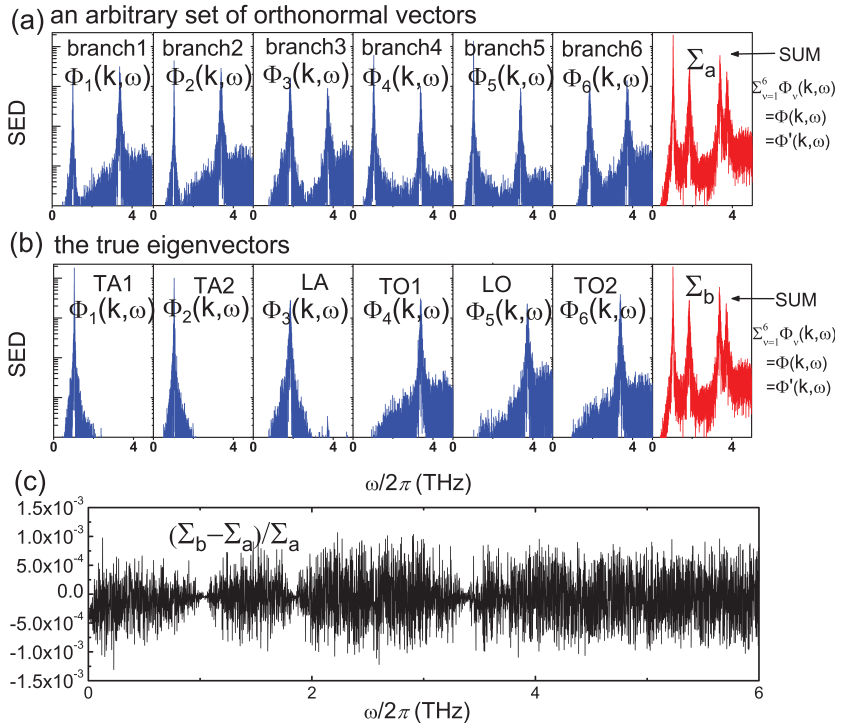

FIG. 4. The SED functions of bulk PbTe calculated based on (a) an arbitrary set of orthonormal vectors and (b) the true eigenvectors at the temperature of 300 K and the reduced wave vector of (0.875, 0, 0). Figure (c) shows the relative difference between the total SEDs given by (a) and (b).

$$\Phi'(\mathbf{k},\omega)=\frac{1}{4\pi\tau_0}\sum_{\alpha,b}^{3,n}\frac{m_b}{N_c}\left|\sum_{l}^{N}\int_0^{\tau_0}\dot{u}_\alpha^{l,b}(t)\exp\left(i\mathbf{k}\cdot\mathbf{r}_0^l-i\omega t\right)dt\right|^2$$
$$=\sum_{\alpha}^{3}\sum_{b}^{n}|\dot{q}_\alpha^b(\mathbf{k},\omega)|^2. \quad (10)$$

In this approach, the eigenvectors are not required.

It has been under debate whether the second version gives the same results with the first version.[21] To find out the relation between Φ (Eq. (8)) and Φ' (Eq. (10)), we write $\dot{q}_{\mathbf{k},\nu}(\omega)$ in vector product format for convenience

$$|\dot{q}_{\mathbf{k},\nu}(\omega)|^2=|\mathbf{e}^\dagger(\mathbf{k},\nu)\,\dot{\mathbf{Q}}(\mathbf{k},\omega)|^2$$
$$=(\mathbf{e}^\dagger(\mathbf{k},\nu)\,\dot{\mathbf{Q}}(\mathbf{k},\omega))^\dagger(\mathbf{e}^\dagger(\mathbf{k},\nu)\dot{\mathbf{Q}}(\mathbf{k},\omega))$$
$$=\dot{\mathbf{Q}}^\dagger(\mathbf{k},\omega)\mathbf{e}(\mathbf{k},\nu)\,\mathbf{e}^\dagger(\mathbf{k},\nu)\dot{\mathbf{Q}}(\mathbf{k},\omega), \quad (11)$$

where superscript "†" denotes complex conjugate and transpose, $\mathbf{e}(\mathbf{k},\nu)$ and $\dot{\mathbf{Q}}(\mathbf{k},\omega)$ are two column vectors defined

$$\mathbf{e}(\mathbf{k},\nu)=[e_1^{b_1}(\mathbf{k},\nu),e_2^{b_1}(\mathbf{k},\nu),\ldots,e_2^{n}(\mathbf{k},\nu),e_3^{n}(\mathbf{k},\nu)]^T \quad (12)$$

$$\dot{\mathbf{Q}}(\mathbf{k},\omega)=[\dot{q}_1^{b_1}(\mathbf{k},\omega),\dot{q}_2^{b_1}(\mathbf{k},\omega),\ldots,\dot{q}_2^{b_n}(\mathbf{k},\omega),\dot{q}_3^{b_n}(\mathbf{k},\omega)]^T, \quad (13)$$

where superscript "T" denotes transpose.

Substitute Eq. (11) into Eq. (8)

$$\Phi(\mathbf{k},\omega)=\sum_{\nu}^{3n}\dot{\mathbf{Q}}^\dagger(\mathbf{k},\omega)\mathbf{e}(\mathbf{k},\nu)\,\mathbf{e}^\dagger(\mathbf{k},\nu)\dot{\mathbf{Q}}(\mathbf{k},\omega)$$
$$=\dot{\mathbf{Q}}^\dagger(\mathbf{k},\omega)\left[\sum_{\nu}^{3n}\mathbf{e}(\mathbf{k},\nu)\,\mathbf{e}^\dagger(\mathbf{k},\nu)\right]\dot{\mathbf{Q}}(\mathbf{k},\omega)$$
$$=\dot{\mathbf{Q}}^\dagger(\mathbf{k},\omega)\,\mathbf{I}\,\dot{\mathbf{Q}}(\mathbf{k},\omega)=\dot{\mathbf{Q}}^\dagger(\mathbf{k},\omega)\dot{\mathbf{Q}}(\mathbf{k},\omega)$$
$$=\Phi'(\mathbf{k},\omega), \quad (14)$$

where $\mathbf{I}$ is a $3n\times3n$ identity matrix. In Eq. (14), we use the orthonormal condition $\sum_\nu^{3n}\mathbf{e}(\mathbf{k},\nu)\,\mathbf{e}^\dagger(\mathbf{k},\nu)=\mathbf{I}$, which is obvious when considering that the dynamic matrix $\mathbf{D}$ is Hermitian: $\mathbf{D}=\mathbf{D}^\dagger$. Analytically, we prove that the total SED function does not depend on eigenvectors and that the second version frequency-domain NMA ($\Phi'(\mathbf{k},\omega)$) gives the same results with the first version ($\Phi(\mathbf{k},\omega)$). This result indicates that any arbitrary set of orthonormal vectors gives the same results of total SED function with the true eigenvectors.

To verify our analytical conclusion, a number of MD simulations are set up for bulk argon, silicon, germanium, and lead telluride. All the results show that Φ and Φ' are exactly the same for the phonon modes. In Fig. 4, we show an example of the SED functions given by (a) an arbitrary set of orthonormal vectors and (b) the true eigenvectors in PbTe at the reduced wave vector of (0.875, 0, 0). The arbitrary set of orthonormal vectors gives different individual-branch SEDs with the true eigenvectors, but they both produce the same total SED. For a clear observation, we plot the relative difference between the total SEDs given by (a) and (b) in Fig. 4(c). The relative difference is within 10^{-3} throughout the frequency range no matter near the peaks or far from the peaks, indicating the difference is zero with the numerical accuracy in the computation. Therefore, the eigenvectors are not absolutely necessary in frequency-domain NMA. In the case that two modes have very close frequencies so that their two SED peaks cannot be distinguished in the total SED plot, applying eigenvector can help to separate them into two individual plots.

IV. CONCLUSIONS

To summarize, the anharmonicity of eigenvector is found, and the role of eigenvector in NMA is discussed. Anharmonic frequency is caused by the change of force constant at finite

temperature, and thus exists in all anharmonic materials. We find that the anharmonicity of phonon eigenvector does exist, but in contrast to frequency, anharmonic eigenvector is caused by the relative change of the different force constants with neighbors of different species and thus only exists in compound materials for which each atom has at least two types of anharmonic interactions with other atoms. This is important to the thermoelectric materials PbTe, PbSe, Bi_2Te_3, etc. As for the role of eigenvector in the frequency-domain NMA, we show that the eigenvectors are unnecessary using both analytical derivations and numerical simulations. This finding can probably resolve the confusion regarding the role of phonon eigenvectors in the frequency-domain NMA. The NMA without phonon eigenvector makes the calculations more convenient and reduces the computational cost. Since eigenvectors are required in time-domain NMA, we expect that the anharmonic eigenvector can improve the computation accuracy in time-domain NMA. The anharmonic eigenvector can find potential use in other areas such as the wave-packet analysis where phonon eigenvectors are required.

ACKNOWLEDGMENTS

We would like to thank Prabhakar Marepalli for sharing the Lorentzian fitting codes. We gratefully appreciate the discussions with Professor Alan J. H. McGaughey and Dr. Jason M. Larkin. Simulations were done at the Purdue Network for Computational Nanotechnology (NCN). The work was partially supported by the National Science Foundation (Award No. 1150948).

[1]A. Shakouri, Annu. Rev. Mater. Res. **41**, 399 (2011).
[2]T. L. Feng and X. L. Ruan, J. Nanomaterials **2014**, 206370 (2014).
[3]D. A. McQuarrie, *Statistical Mechanics* (University Science Books, Sausalito, 2000).
[4]A. A. Maradudin and A. E. Fein, Phys. Rev. **128**, 2589 (1962).
[5]A. A. Maradudin, A. E. Fein, and G. H. Vineyard, Phys. Status Solidi. **2**, 1479 (1962).
[6]M. Omini and A. Sparavigna, Phys. Rev. B **53**, 9064 (1996).
[7]M. Omini and A. Sparavigna, Physica B **212**, 101 (1995).
[8]A. J. C. Ladd, B. Moran, and W. G. Hoover, Phys. Rev. B **34**, 5058 (1986).
[9]A. J. H. McGaughey and M. Kaviany, Phys. Rev. B **69**, 094303 (2004).
[10]C. Z. Wang, C. T. Chan, and K. M. Ho, Phys. Rev. B **40**, 3390 (1989).
[11]J. Shiomi and S. Maruyama, Phys. Rev. B **73**, 205420 (2006).
[12]N. de Koker, Phys. Rev. Lett. **103**, 125902 (2009).
[13]J. A. Thomas, J. E. Turney, R. M. Iutzi, C. H. Amon, and A. J. H. McGaughey, Phys. Rev. B **81**, 081411(R) (2010).
[14]J. A. Thomas, J. E. Turney, R. M. Iutzi, A. J. H. McGaughey, and C. H. Amon, in *Proceedings of the 14th International Heat Transfer Conference* (ASME, 2010), paper no. IHTC14-22262.
[15]B. Qiu, H. Bao, G. Zhang, Y. Wu, and X. Ruan, Comput. Mater. Sci. **53**, 278 (2012).
[16]J. E. Turney, E. S. Landry, A. J. H. McGaughey, and C. H. Amon, Phys. Rev. B **79**, 064301 (2009).
[17]B. Qiu and X. Ruan, Appl. Phys. Lett. **100**, 193101 (2012).
[18]S. Maruyama, Nanoscale Microscale Thermophys. Eng. **7**, 41 (2003).
[19]A. S. Henry and G. Chen, J. Comput. Theor. Nanosci. **5**, 1 (2008).
[20]J. V. Goicochea, in IEEE/CPMT 26th Semiconductor Thermal Measurement, Modeling & Management Symposium (SEMI-THERM) (IEEE, 2010), pp. 278.
[21]J. M. Larkin, J. E. Turney, A. D. Massicotte, C. H. Amon, and A. J. H. McGaughey, J. Comput. Theor. Nanosci. **11**, 249 (2014).
[22]J. D. Gale and A. L. Rohl, "The general utility lattice program," Mol. Simul. **29**, 291 (2003).
[23]S. Plimpton, "Fast parallel algorithms for short-range molecular dynamics," J. Comput. Phys. **117**, 1 (1995).
[24]L. T. Kong, Comput. Phys. Commun. **182**, 2201 (2011).
[25]L. Porter, J. Li, and S. Yip, J. Nucl. Mater. **246**, 53 (1997).
[26]J. Li, L. Porter, and S. Yip, J. Nucl. Mater. **255**, 139 (1998).
[27]J. Tersoff, Phys. Rev. Lett. **64**, 1757 (1990).
[28]J. Tersoff, Phys. Rev. B **49**, 16349 (1994).
[29]M. T. Dove, *Introduction to Lattice Dynamics* (Cambridge University Press, New York, 1993).